Materials Chemistry and Physics 258 (2021) 123677

Contents lists available at ScienceDirect

Materials Chemistry and Physics

journal homepage: www.elsevier.com/locate/matchemphys

Carboxymethyl cellulose sizing repairs carbon fiber surface defects in epoxy composites

Baowei Qiu, Muxuan Li, Xueqin Zhang, Yang Chen, Shengtai Zhou, Mei Liang **, Huawei Zou *

The State Key Lab of Polymer Materials Engineering, Polymer Research Institute of Sichuan University, Chengdu, 610065, China

HIGHLIGHTS

- Repaired the surface defects of carbon fiber to reinforce epoxy-based composites.
- Increased the body strength of carbon fiber and chemical bonding strength between the fibers and the matrix.
- The interfacial shear strength (IFSS) of the composites increased by about 18%.
- Analyzed the influence of the distribution of carbon fiber in the matrix on the composites.

GRAPHICAL ABSTRACT

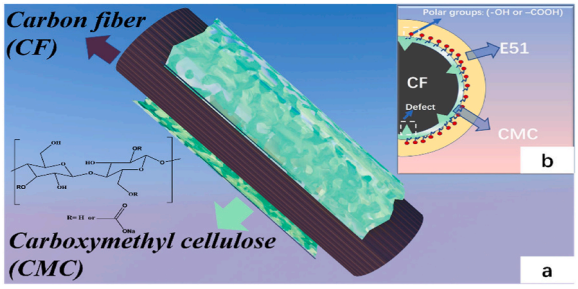

ARTICLE INFO

Keywords:
Carbon fiber
Carboxymethyl cellulose
Interface
Epoxy

ABSTRACT

Carbon fiber inevitably generates a large number of defects coupling with the multi-functional groups on its surface during the production process. As a result, these defects will cause stress concentration at the interface, thereby reducing the performance of carbon fiber reinforced polymer composites (CFRPs). In this work, a self-driven method is adopted to repair the surface defects of CFs to improve the interface properties of CFRPs. The surface of CFs is sized by nano-carboxymethyl cellulose (CMC) with multi-functional groups. Due to the existence of multi-functional groups on the surface defects of CFs and the non-polarity of other areas in CFs, CMC can automatically gather at the defects via polar attraction between the multi-functional groups to achieve the self-driven repair. Besides, due to the film-forming properties of CMC, the surface defects will be used as a fixed points to form a tight layer of nanofiber membrane with the multi-functional groups on the surface of CFs. It is found that the repair of CFs surface defects and the introduction of multi-functional groups will synergistically enhance the interface performance of epoxy-based composite. The modification method is environmental benign, which lays a research foundation for improving the interface properties of CFRPs using natural cellulose.

1. Introduction

As advanced composites, carbon fiber reinforced polymer composites (CFRPs) are widely used in mechanical engineering [1,2], aerospace [3,4], automotive industries [5] because of their excellent mechanical performance to weight ratio [6,7]. Generally, the interface between carbon fibers (CFs) and resin is pivotal for the mechanical performance of CFRPs, because the load is transferred from resin to CFs to reduce the

* Corresponding author.
** Corresponding author.
E-mail addresses: liangmeiww@163.com (M. Liang), hwzou@163.com, hwzou@163.com (H. Zou).

https://doi.org/10.1016/j.matchemphys.2020.123677
Received 4 June 2020; Received in revised form 11 August 2020; Accepted 12 August 2020
Available online 19 September 2020

stress concentration induced by the interface [8–10]. Better interphase properties often provide a better mechanical performance of composites [11,12]. However, the number of polar groups on the surface of untreated CFs is small resulting in a weak interaction with resin matrix [13]. Beside, CFs as the rigid material, due to the existence of surface defects, when the CFRPs are subjected to stress, it is easy to cause stress concentration at the interface, resulting in a decrease of their material performance [14,15]. These questions restrict the further improvement of CFRPs' performance and have become a long-existing critical issue for the development of them. Therefore, the modification of CFs to obtain an excellent interface is of great significance to realize the high performance of CFRPs and solve the future demand for advanced composite materials.

The interfacial properties relate to the chemical composition and morphology of CFs surface [16,17]. CFs will inevitably cause a large number of defects with multi-functional groups during the production process, and these defects have a crack tip effect and produce stress concentration at the interface [18–20]. Many researchers focused on modifications of CFs inert surface to introduce additional chemical reactive sites and surface areas for adhesion to make CFs/resin interfacial properties better, such as sizing [21–25], grafting [13,26], chemical vapor deposition [27–29], electrochemical method [30–32], plasma treatment [33–35], etc. However, it has been recognized that strong (chemical) treatment may damage the surface of CFs, resulting in even greater defects, thereby reducing its mechanical properties [36,37]. In order not to damage the strength of the CFs body and cause more defects, we used the multi-functional groups at the defects on the surface of CFs as a breakthrough point to enhance the interface performance of the composite material. During the sizing process, taking advantage of the difference between the multi-functional groups of CFs defects and the surface inertness, particles with polar groups will automatically adsorb to the defects according to the infiltration theory [38–40]. Furthermore, nanoparticles with polar groups on CFs will also effectively weaken the crack tip effect of CFs and enhance the tensile strength of CFs and the comprehensive properties of CFRPs [20,41]. Sizing is considered as the best method to improve the interface properties without damaging the mechanical properties of CFs [42]. It also can tailor the wettability and improve the reactivity of CFs without the complicated chemical reaction or grafting [43,44].

Because of nanometer size and multi-functional groups, carboxymethyl cellulose (CMC) is an appropriate choice as the emulsion sizing agent to improve interface properties [45,46]. The glucopyranose ring of CMC has an abundant hydroxyl group, which can improve the surface wettability of CFs [47,48]. There are a lot of oxygen-containing functional groups on the surface defects of CFs [40]. During the sizing process, nano CMC will automatically be adsorbed on the defects to fill them and increase the radius of the crack tip. It can effectively avoid the stress concentration of the crack tip and improve the mechanical performance of CFRPs [49]. Besides, due to the film-forming properties of CMC, the defects will be used as a fixed point to form a tight layer of nanofiber membrane with the multi-functional groups on the surface of CFs. The polyfunctional group membrane will act as a bridge between CFs and epoxy (EP) to improve the interface performance of CFRPs. Furthermore, a variety of functional structural materials can be prepared by combining CMC and carbon materials including carbon nanotubes, graphene, carbon black, etc [50–52]. Hence, the application of these materials in CFRPs also relies on the study of CMC improving the interface properties between CFs/matrix.

In this paper, we hope to improve the mechanical properties of the CFRPs via self-driven repair of the surface defects of CFs with nano-scale CMC and introduce polar functional groups onto the surface of CFs. And the effects of different concentrations of CMC on the interface properties between CFs and EP were investigated. And the effects of these physical and chemical modifications on surface morphology, surface chemical composition, monofilament tensile strength of CFs, dynamic wettability, and interfacial adhesion between CFs and epoxy were compared and studied.

2. Experiments

2.1. Materials

The PAN-based carbon fibers without a sizing agent (average diameter 7 μm, linear density 0.404, density 1.78 g/cm^3) were supplied by Heng Shen Industries, Inc. (Jiangsu, China). The carboxymethyl cellulose (CMC, 50–100 MPa s, DS = 0.7) was purchased from Aladdin Reagent Industries, Inc. (Shanghai, China). The epoxy used was Bisphenol-A type epoxy resin (E51, epoxy value 0.49–0.54 mol/100g), and obtained from De Yuan Epoxy Technology Industries, Inc. (Shandong, China). The curing agent was 4,4′-diamino diphenylmethane (DDM) and provided by Aladdin Reagent Industries, Inc. (Shanghai, China). All reagents can be used directly and do not need to be purified.

2.2. Methods

2.2.1. CFs modification

100 g deionized water was added to each of the five 200 mL beakers. 0 g, 0.0250 g, 0.050 g, 0.0750 g, 0.1000 g CMC was added into them, respectively. Stirring for 2 h to disperse the CMC evenly in the water. Take a 5-m-long piece of CF to wrap around a frame (4 cm × 8 cm) made of polytetrafluoroethylene (PTFE) and then five of them were placed into the above five beakers individually. This means the 5-m-long piece of CF (weight about 2.02 g) was treated by 0 g, 0.0250 g, 0.050 g, 0.0750 g, 0.1000 g CMC, respectively. The CF samples were dipped sizing for 10 min and dried in a vacuum oven at 40 °C for 24 h. The samples after the above series processes were named as CF, CF/0.025 g CMC, CF/0.050 g CMC, CF/0.075 g CMC, CF/0.010 g CMC, respectively.

2.2.2. Preparation of composites

The modified CFs, E51 resin, and curing agent DDM were used to prepare CFRPs. Equal amounts of E51 and DDM were mixed in a beaker and stirred by an agitator in the oil bath for 15 min at 80 °C. Then the CFs with a length of 5 m were wrapped by the epoxy and put into the mold. After that, the samples were cured at 135 °C under 10 MPa for 2 h and 175 °C for 2 h under 10 MPa, respectively. Composite laminates were obtained with about 62 vol % CFs (width and thickness of specimens: 6.5 mmm × 2 mm) for tests.

3. Results and discussion

3.1. Chemical characterization of CFs surface

3.1.1. FTIR analysis

The chemical structure of the materials is obtained by FTIR (Fig. 2). From Fig. 1, it can be seen the chemical structure of CMC in Fig. 1. The FTIR data shows CMC may be successfully sized on the surface of CFs and there are no chemical reactions between CFs and CMC when they were combined. As shown in Fig. 2, the peak of 3385 cm^{-1} is assigned to the stretching vibration of –OH group or hydrogen bond. Water molecules in the environment attached to the surface of CFs, causing the –OH peak of CFs [53]. However, the peak of 3385 cm^{-1} of CMC comes from the hydroxyl functional group and hydrogen bonding. The presence of hydrogen bonds of CMC may be the reason that the peak width of the mixture is wider than that of CFs. The characteristic absorption bands in the range of 1620–140,1200-1000 cm^{-1} were attributed to the stretching vibrations of –COO and -C-O- on the polysaccharide skeleton. This result is consistent with previous reports [54,55]. And we think the peak of 600–900 cm^{-1} may be the fingerprint area of CMC which was caused by its glucose structure. Further, the characteristic peak of CMC appears and no other new peak occurs on the modified surface of CFs. In summary, CMC may attach to the surface of CFs to increase functional groups by sizing and the process is a physical process.

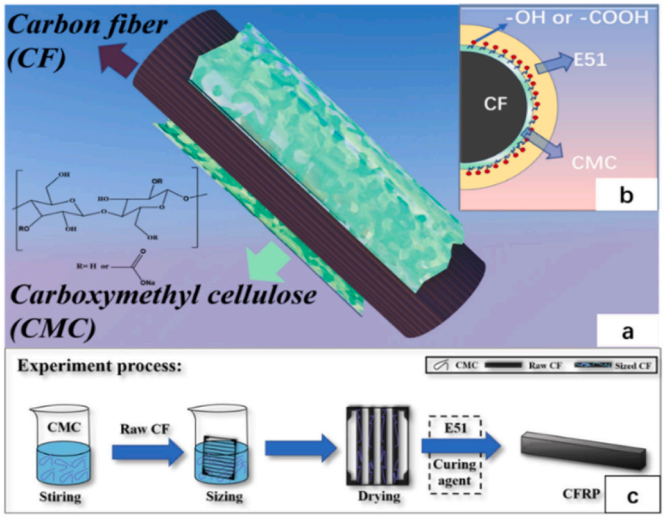

Fig. 1. (a) Illustration of the preparation of modified CFs, (b) the preparation structure of CFRPs and (c) illustration of the experimental process of modified CFRPs.

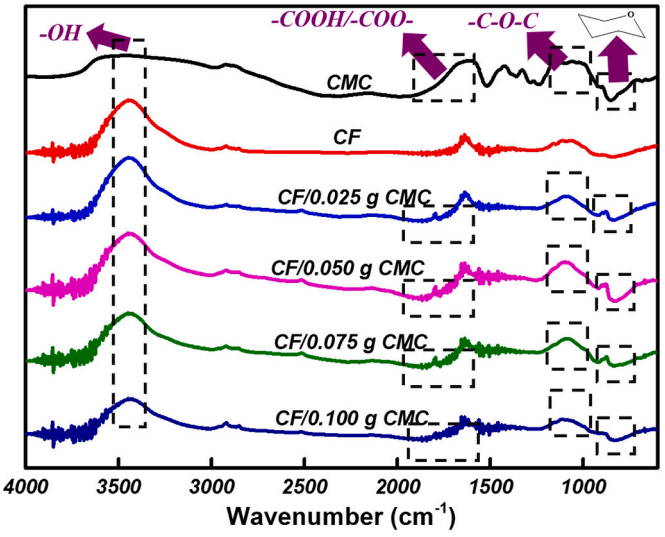

Fig. 2. FTIR spectra of CMC, CF, CF/0.025 g CMC, CF/0.050 g CMC, CF/0.075 g CMC, CF/0.100 g CMC.CFs were analyzed by FTIR spectrophotometer using powder-pressed KBr tablets. The CFs were cut as short as possible and ground into powder with KBr for FTIR measurements.

3.1.2. Raman spectrum analysis

The structure changes on the surface of CFs were analyzed by Raman spectroscopy. It can be seen from Fig. 3 (a) that the Raman spectral regions of CFs after different treatments have two obvious spectral lines: the D line (disordered carbon structure: 1360 cm^{-1}) and G line (graphite crystallite structure: 1580 cm^{-1}) [56]. R ($R = I_D/I_G$) is the integrated intensity ratio of the D line (the disordered structure) to the G line (the graphite structure), and it was used to measure the change of the surface defects and the low symmetrical structure of CFs [57]. The smaller the R-value was, the higher the degree of graphitization of the carbon fiber was, and the higher the degree of ordering of the crystallites was. The value of $I_D/(I_D + I_G)$ indicates the relative content of microcrystalline defects in carbon materials.

As seen from Table 1, compared to that of the untreated CFs, the position of D and G line of the treated CFs slightly shifts towards the higher wavenumber, and the half-width of D line of the treated CFs is increased, while the half-width of G-line is opposite. This indicates that the graphite crystallite structural performance of carbon fiber tends to be stable, contrary to the disordered carbon structure. From Fig. 3 (b), we can see the graphitization degree of T300, which overlaps relative to peak D and peak G, while the intensity of peak D is greater than that of peak G, indicating that the disordered structure of T300 is greater than the graphite structure. Thus the main structure of T300 is chaotic graphite structure instead of complete graphite structure. With the gradual addition of cellulose, the R and $I_D/(I_D + I_G)$ value also gradually increased, indicating that the degree of fiber defects and the relative content of it, on the whole, is gradually increasing. The increase in active defects will improve the interface bonding strength of the CF/EP.

3.2. Surface morphology of CFs

From Fig. 4 (a), the untreated CFs are dispersed in the macroscopic morphology. With the addition of CMC, CFs bundling gradually increases, indicating that CMC has a positive effect on CFs bundling. From the microscopic morphology of Fig. 5 (b), the untreated surface of CFs has small grooves parallel to the fiber axis due to the spinning process of the CFs precursor and presents a neat and smooth appearance. There are also a few local protrusions and pits on the surface of untreated carbon fiber, which form certain physical defects and easily cause stress concentration during use. After sizing, CFs appear to be closely bound with cellulose film, which may due to the emulsification of CMC on the surface of CFs and improves the interface bonding. With an increase of CMC content, the surface grooves become shallower, and the morphology is no longer neat and smooth, and CMC film-forming on the surface of CFs causes protrusions and wrinkles. These rough morphology can increase the area of contact between CFs and the resin matrix. According to the mechanical locking theory, it may help the CF/matrix combination. When CMC is increased to 0.075 g, as seen in Fig. 4 (e), the cellulose film begins to form between the fibers, and fiber bonding occurs. When the content of CMC is 0.100g, as shown in Fig. 4 (f), large-scale films formed on the surface of CFs, and bonding phenomena occur among CFs. This phenomenon may block the epoxy resin infiltration channel, and reduce the contacting surface area between CFs and epoxy, reducing the mechanical performance of the composite subsequently.

The morphology and average roughness of the CFs' surface are measured by AFM. It can be seen from Fig. 4 (g) that the untreated surface of CFs exhibits a wide and smooth sheet-like morphology. Those grooves parallel to the fiber axis on the surface in the scanning electron microscope can also be seen in the AFM. After sizing, the microstructure of CFs surface changed and the average roughness increased. According to current research, higher roughness often leads to better interface performance [58,59]. From Fig. 4(g–k), we can see that the average roughness increased from 21 to 89 as the sizing concentration increased. This may be due to the small molecules of the slurry after sizing immersed in the grooves on the surface of CFs, and the large molecules form film prominent on the surface of CFs. As the content of CMC increases, the area, and thickness of the film increase. Furthermore, due to the uneven surface tension during the film formation of cellulose, uneven protrusions will be formed, resulting in the average roughness gradually increased. The phenomenon can be presented in Fig. 4 (e) and (f). From Fig. 4 (l), and we can see that compared with untreated CFs, the surface of modified CFs has a larger number of protrusions and a greater height difference. These active protrusions with a certain height will help to bond with EP and improve the interface properties.

3.3. Modified strength analysis

3.3.1. Monofilament tensile strength of CFs

In resin matrix composites, CFs play an important role in load-bearing because the strength of the fiber is much higher than that of resin [60]. The mechanical strength of CFs directly affects the mechanical properties of CFRPs. Fig. 5 shows the single fiber tensile strength of CFs with different content of CMC. It is necessary to

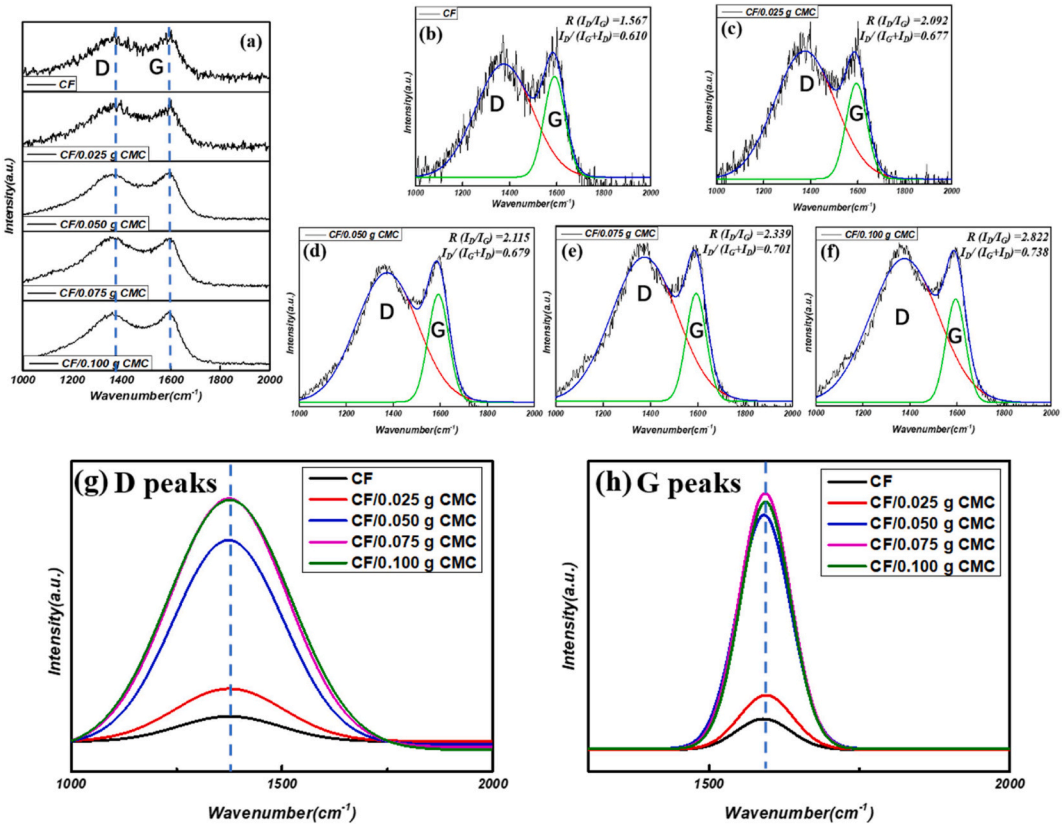

Fig. 3. Raman spectra curves were fitted by the Gaussian function: (a) full spectra, (b) CF, (c) CF/0.025 g CMC, (d) CF/0.050 g CMC, (e) CF/0.075 g CMC, (f) CF/0.100 g CMC showing the contribution from the two main modes D and G, (g) D peaks of all samples, (h) G peaks of all samples. Raman spectrometer used a helium-neon laser to emit a laser with a wavelength of 633 nm and scanned the surface of CFs in the range of 500–3000 cm^{-1} through a grating of 600 gr/mm.

Table 1
Comparison of Raman peaks of samples.

Samples	D Peak		G Peak		R (ID/ IG)	$I_D/(I_G + I_D)$
	Peak position (cm^{-1})	Half-height width (cm^{-1})	Peak position (cm^{-1})	Half-height width (cm^{-1})		
CF	24808	284	15836	105	1.567	0.610
CF/ 0.025 g CMC	42652	302	20392	104	2.092	0.677
CF/ 0.050 g CMC	161525	307	76359	103	2.115	0.679
CF/ 0.075 g CMC	205968	326	88048	99	2.339	0.701
CF/ 0.100 g CMC	198020	341	70165	97	2.822	0.738

understand the change of CFs tensile strength before and after sizing, which is helpful to analyze the effect of CMC on the strength of CFs body [61]. WEIBULL modulus m characterizes the uniformity and reliability of the single filament strength of CFs and the higher m value indicates the higher uniformity and reliability of CFs [62]. We can see from Fig. 5 the m value of treated CFs is higher than that of untreated CF, which means CMC sizing CFs can effectively increase the uniformity and reliability of CFs and their single filament strength. And we have noticed that with the increase of CMC content, the m value of CFs has been increasing until the addition amount reaches 0.100 g. Next, we will explore the reason by observing the fiber morphology through the optical microscope.

CFs are the brittle material. According to the Griffith micro-crack theory, when subjected to external forces, CF tends to form stress concentration at the crack tip and release it with the value-added and expansion of the crack [63]. It often results in fractures under low stress, which is also the preliminary cause of carbon fiber strength dispersion. The crack propagation force depends on the shape, size of the crack body, its load-bearing method, the location of the crack, the shape and size of the defect, etc [64]. There are many defects on the surface of CFs, and there are a large number of oxygen-containing free radical groups such as hydroxyl groups and oxides at these defects. During the sizing process in Fig. 6 (e), the polar groups of CMC will preferentially adsorb on the oxygen-containing functional groups of these defects to fill the defects and pores on the surface of CFs. The presence of CMC will increase the radius of the crack tip and avoid stress concentration at the defect. Meanwhile, under the action of external force, the shear action between CMC and CFs will also consume part of the load [40,49]. All of these will repair defects and share the load to CFs, and ultimately increase the tensile strength of CFs. Under the microscope in Fig. 6(a–e), we can see that the diameter of CFs increases through the increase of the sizing content. When the addition amount reaches 0.100 g, a large number of uneven bumps appear on the surface of CFs. Combined with the crack tip theory, this may be the value of m becomes smaller and the cause of performance dispersion.

3.3.2. *Contact angle of CFs*

Good wettability is a necessary condition for two-phase carbon fiber composite material to achieve good bonding. The wettability of the surface of the single carbon fiber was determined by the contact angle measurement according to the principle of surface physical chemistry [65]. At the moment when the fiber surface is in contact with the liquid,

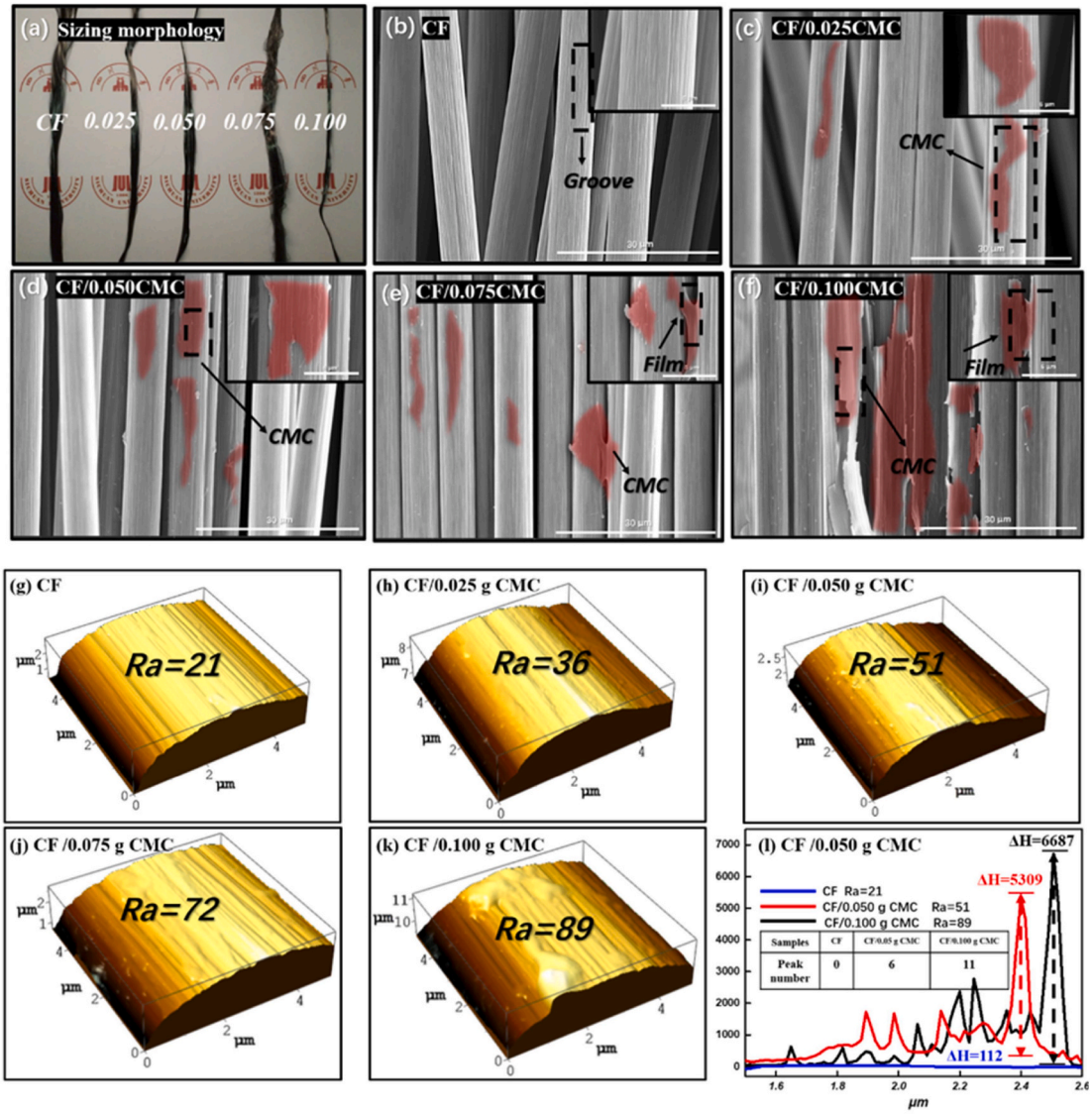

Fig. 4. CFs sizing picture(a) and SEM of CFs surface of (b) CF, (c) CF/0.025 g CMC, (d) CF/0.050 g CMC (e) CF/0.075 g CMC(f) CF/0.100 g CMC. AFM of CFs surface of (g) CF, (h) CF/0.025 g CMC, (i) CF/0.050 g CMC (j) CF/0.075 g CMC(k) CF/0.100 g CMC and (l) the analysis of sample peaks.

a strong adsorption force generates and the contact point is moved, resulting in a small contact angle [66]. Therefore, the smaller the contact angle is, the better the wettability of the carbon fiber is. Conversely, the wettability of the carbon fiber is poorer. It can be seen from Fig. 7(a) the contact angle of untreated CFs is 120.4°, indicating that the wettability of untreated CFs is poor, which is related to its inert surface and the small number of polar functional groups. In Fig. 7(f), as the CMC content increases, the water contact angle decreases significantly. When CMC content is 0.100 g, the water contact angle is 85.9°, which is about 1/3 lower than that of untreated CF. Combining infrared spectroscopy (Fig. 2) and Raman spectroscopy (Fig. 3) analysis, the introduction of polar functional groups such as hydroxyl carboxyl groups on the CMC increases the polarity is the main factor that causes the surface energy of the CFs to reduce the water contact angle. Therefore, CMC has a positive effect on CFs surface wettability. And from the above point of view, higher addition of CMC seems to have a better improvement effect on the interface between CFs/EP.

3.3.3. *ILSS of CFRPs*

As one of the most important properties of CFRPs, ILSS can directly reflect the interfacial properties of CFRPs. In Fig. 8 (a), the ILSS of unmodified CFs is 41.67 MPa. As the content of CMC increases, the ILSS of CFRPs also increases. When the added amount of CMC added reaches 0.075 g, the maximum value of ILSS reached 49.21 MPa. Combined with the above test results, it may be the introduction of polar functional groups, and the increase of the surface roughness of the fiber synergistically improve the interface properties of CFs/matrix, and then improve the ILSS of the composite. However, when the amount of CMC is 0.100 g, ILSS of the composite is 42.15 MPa. The interfacial properties of the composite material decreased with the increase of CMC content. This may be due to the increase of CMC content seen in the SEM, which further increased the adhesion between the fibers and blocked the epoxy infiltration channel. As a result, the epoxy resin does not fully permeate into the CFs, resulting in the performance degradation of the composites. Therefore, ILSS increases with the increase of its content only when CMC is added in an appropriate amount, and CMC has a positive effect on enhancing the interface bonding force between CFs/matrix.

As can be seen from Fig. 8 (b) and (c), compared with the unmodified CFs, the ILSS of the composite material with an added amount of 0.075 g increased by about 7.5 MPa, and the enhancement was about 18%. Compared with the reported modification results using GO as the sizing agent, the enhancement range of adding 0.075 g CMC is more than 6%,

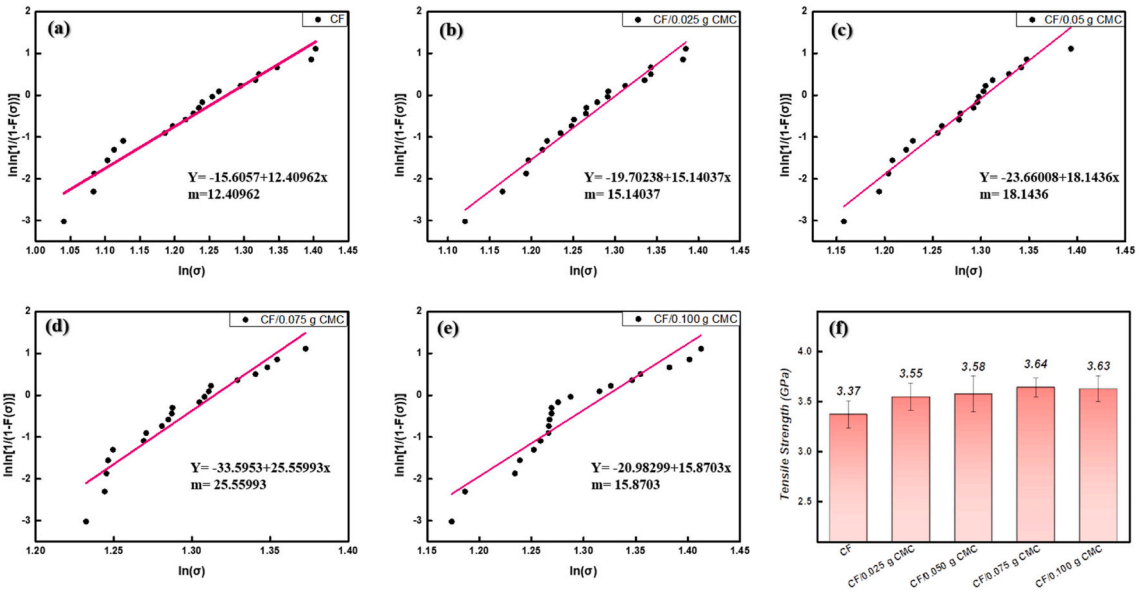

Fig. 5. Linear fit graph of CFs WEIBULL:(a) CF, (b)CF/0.025 g CMC, (c)CF/0.050 g CMC, (d)CF/0.075 g CMC, (e)CF/0.100 g CMC and CFs monofilament tensile strength.

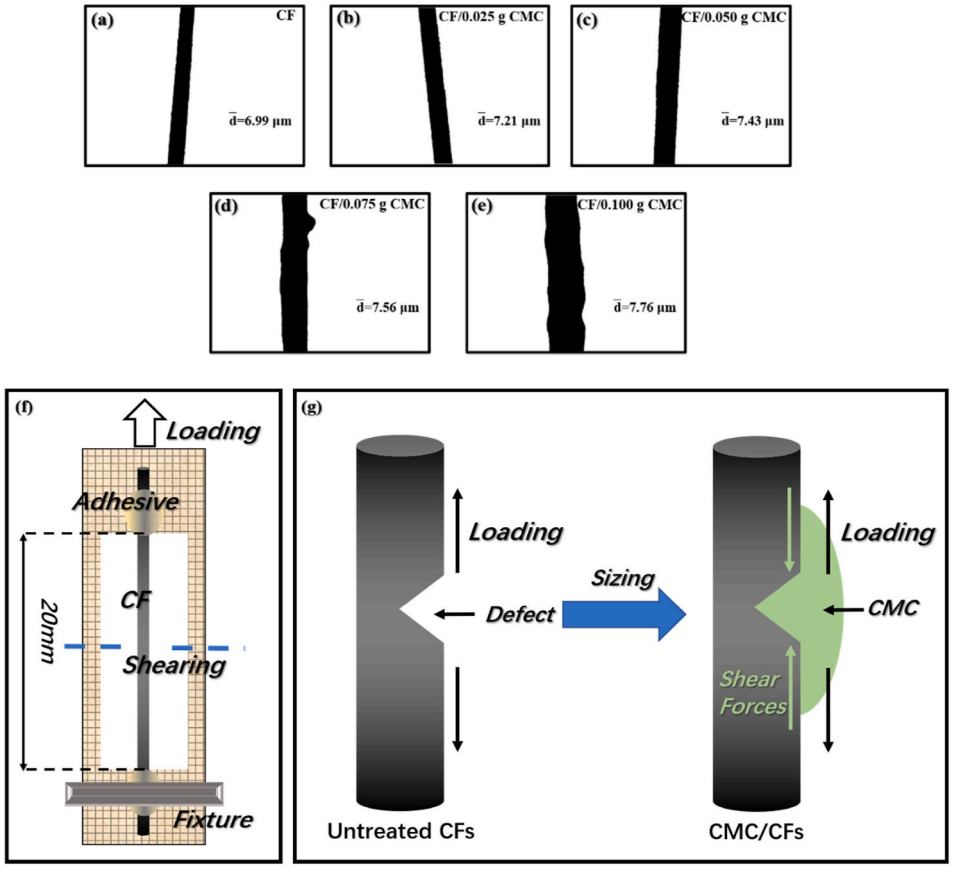

Fig. 6. Microscope image of (a) CF, (b)CF/0.025 g CMC, (c)CF/0.050 g CMC, (d)CF/0.075 g CMC, (e)CF/0.100 g CMC. (g)schematic diagram of making monofilament tensile samples and (f)Schematic diagram of fiber surface changes before and after sizing.

and the absolute value is about 2 MPa higher. Besides, compared with the lignin enhancement effect of the same type, its enhancement amplitude is not as good as that of lignin, which is mainly due to the low strength of the carbon fiber body used by lignin. However, the absolute value of CMC modification enhanced value is 2 MPa higher than lignin. Therefore, CMC may be a better choice than GO and lignin in the interface properties of sizing modified CFs/matrix. To further understand its interlayer failure mechanism, the morphology of its longitudinal and cross-section fractures will be analyzed.

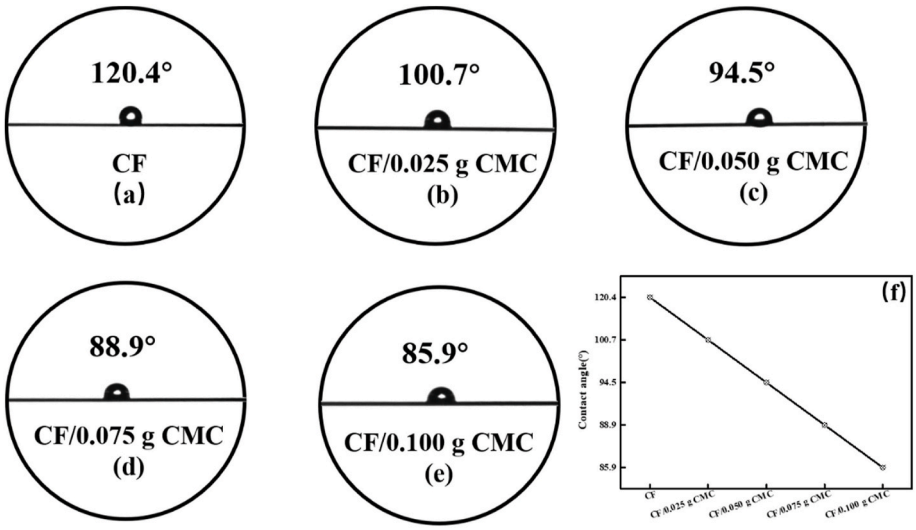

Fig. 7. Contact angle of (a) CF, (b)CF/0.025 g CMC, (c)CF/0.050 g CMC, (d)CF/0.075 g CMC, (e)CF/0.100 g CMC. (f) line chart of contact angle change.

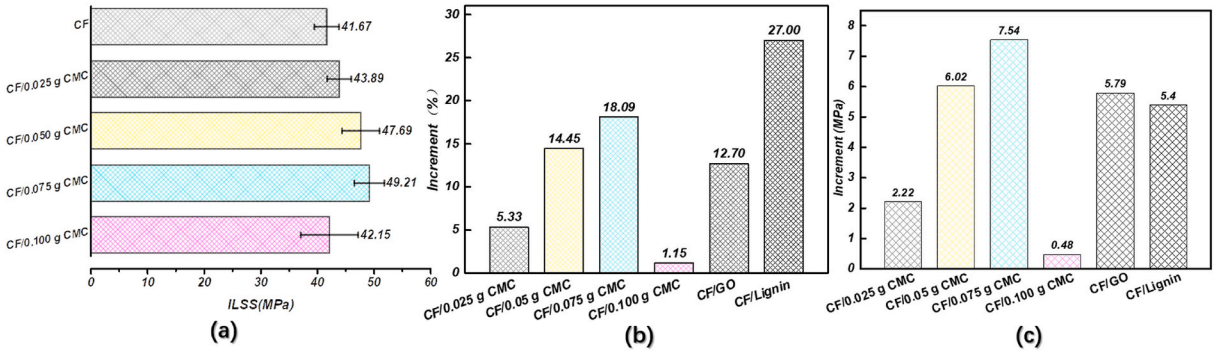

Fig. 8. The ILSS comparison of modified CF (a), the ILSS comparison with literature composites (b): increment (%), (c): increment (MPa), literature composites: CF/GO [67] and CF/Lignin [68].

3.4. Interfacial fracture morphology of CFRPs

The morphology of the longitudinal section (parallel to the axial direction of CF) and crossection (vertical to the axial direction of CF) of the composites were characterized by SEM, as seen in Fig. 9. The morphology of the untreated CFs longitudinal section can be seen in Fig. 9 (a). The surface of untreated CFs is clean and complete after the CFRP is broken, and almost no epoxy remains on it. Due to the weak interface bonding force between CFs and epoxy, epoxy cannot attach well to the surface of CFs when the CFRP is broken. The break mainly occurs at the interface between CFs and epoxy because the stress cannot be transferred from the matrix to the CFs. It can be seen from Fig. 9 (b) that when the amount of CMC added is 0.075 g, the amount of epoxy residue on the surface of the fiber increases significantly after brerface. Then the fiber bears the stress and breaks, which reveals that CMC can effectively improve the interface bonding strength of CFs/epoxy and achieve the effect of transferring stress. However, when the CMC content is further added to 0.100 g, CFRPs show a bonding morphology after breaking. Combined with the SEM in Fig. 4 (b), this should be caused by the phenomenon of CFs sizing bonding. As a result, the epoxy cannot be infiltrated between CFs, which results in insufficient epoxy infiltration and reduces the strength of the composite.

From the longitudinal cross-sectional morphology of unmodified fibers in Fig. 9 (a'), we can see that when CFs and the substrate are peeled off, CFs are pulled out as a whole due to the weak interface adhesion between CFs and epoxy, leaving a lot of holes. However, when the amount of CMC added is 0.075 g, no CF is pulled out from the longitudinal section in Fig. 9 (b'). like the cross-section. CFs have cracks and fractures caused by load-bearing stress. The morphological break also appears in the samples with the CMC addition amount of 0.100 g in Fig. 9 (c'). Combined with Fig. 4 (c), we think CMC has a positive effect on enhancing the interfacial bonding between CF and epoxy. The high concentration of CMC seems to have little effect on the transfer of interfacial stress. The decrease of CFRPs' performance is caused by the insufficient infiltration of CFs with epoxy.

To understand the modification of CMC to CFs and EP more intuitively, we conducted a statistical analysis of the distribution of CFs in the longitudinal profile of CFRPs broken. The pictures of SEM are divided into 64 squares, and the number of fibers in each square is indicated by the color depth. From the statistical analysis chart, we can see that the distribution interval of unmodified CFs in the composite material is large. There are many light-colored parts, and the arrangement is relatively loose. Besides, we can also see from the pictures that the fibers after sizing are arranged closer than those without sizing, and the number of fibers in each rectangle increases from 1–2 to more than 2 as the cellulose content increases. This is consistent with its macroscopic morphology. As the cellulose content increases, the overall distribution color becomes darker, indicating that the fibers are arranged more closely. It can be seen that when 0.100 g is added, about 90% of the fibers are containing two or more fibers, and the fiber arrangement is to tightening will block the epoxy infiltration channel, which is conducive to the performance of CFRPs.

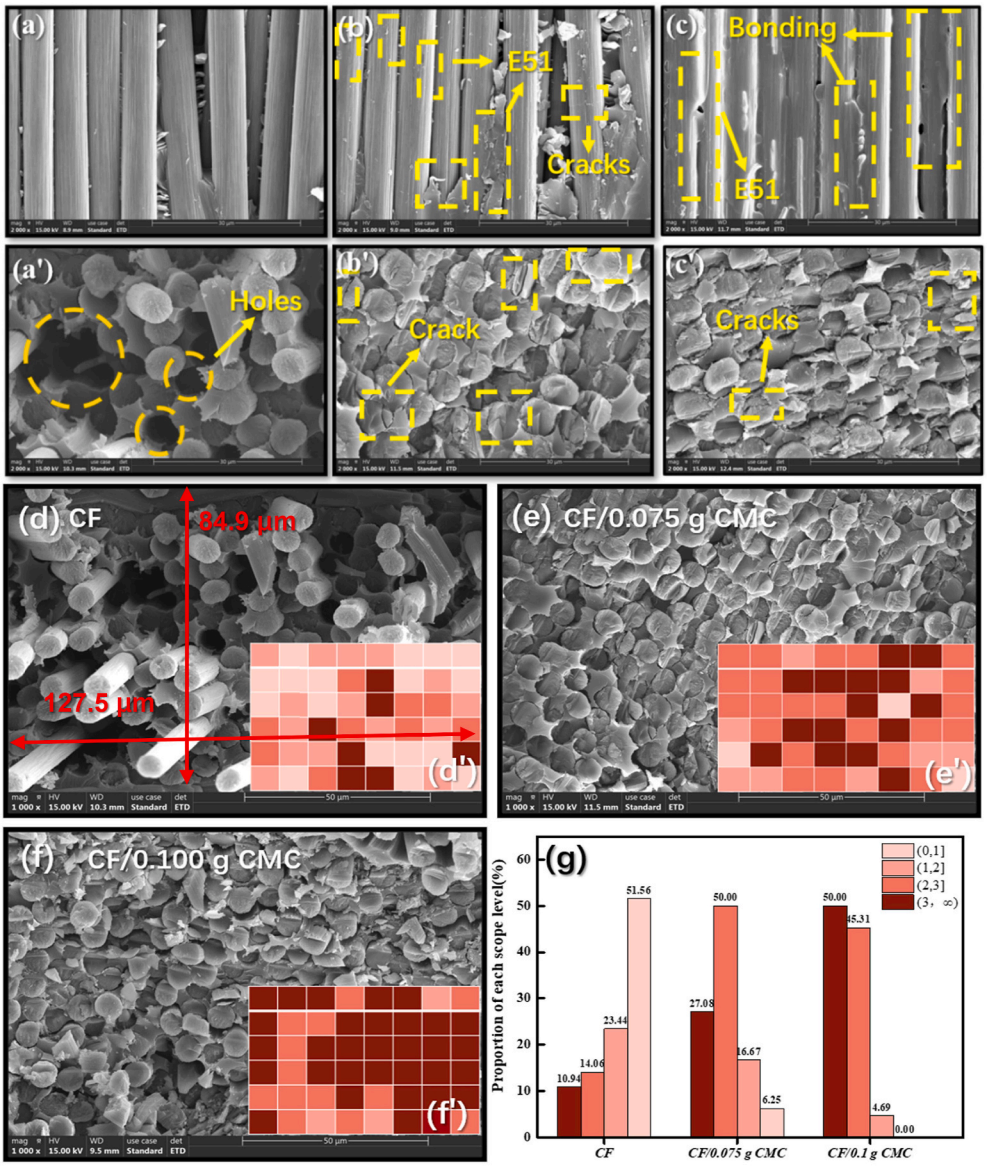

Fig. 9. SEM photos of the longitudinal section (parallel to axial direction of CF): (a) CF, (b) CF/0.075 g CMC, (c) CF/0.100 g CMC and crossection (vertical to axial direction of CF): (a') CF, (b') CF/0.075 g CMC, (c') CF/0.100 g CMC. SEM photos of the crossection (vertical to axial direction of CF): (d) CF, (e) CF/0.075 g CMC, (f) CF/0.100 g CMC, fiber count:(d') CF, (e') CF/0.075 g CMC, (f') CF/0.100 g CMC and (g) statistical analysis. The length and the width of each rectangle is 15.94 μm and 14.15 μm in (d') CF, (e') CF/0.075 g CMC, (f') CF/0.100 g CMC.

4. Conclusion

In this study, the surface of CFs was modified with CMC via the self-driven repair mechanism and results showed that both the strength and interface properties of CFs/EP composites were greatly improved. When the amount of CMC added is 0.075 g, the interface properties of CFRPs are the best. The ILSS of the modified CFRPs increased by approximately 8 MPa when compared with that of the untreated counterparts. The introduction of CMC can repair defects of CF and weaken the stress concentration of the crack tips of CFs to enhance the strength of the monomer. It can also introduce polar functional groups to increase the surface polarity and improve the interface properties between CFs and EP. Also, an excessive addition of CMC will affect the distribution of CFs in CFRPs and the penetration of EP into the CFs, thereby deteroprating the performance of the composite material. In summary, the modification method has the advantages of not damaging CF and being environmentally friendly, which lays a research foundation for improving the interface properties of CFRPs with natural cellulose.

CRediT authorship contribution statement

Baowei Qiu: Writing - original draft, Visualization, Investigation, Conceptualization. **Muxuan Li:** Supervision, Investigation, Conceptualization. **Xueqin Zhang:** Writing - review & editing, Investigation. **Yang Chen:** Writing - review & editing, Supervision. **Shengtai Zhou:** Writing - review & editing, Supervision. **Mei Liang:** Writing - review & editing, Visualization, Supervision, Investigation, Conceptualization. **Huawei Zou:** Funding acquisition, Project administration, Conceptualization.

Declaration of competing interest

The authors declare that they have no known competing financial interests or personal relationships that could have appeared to influence the work reported in this paper.

Acknowledgment

The authors thank the National Natural Science Foundation of China (51703137) and the Fundamental Research Funds for the Central

Universities of China (2015SCU11008) for financial support. We also appreciate Hui Wang from the Analytical & Testing Center of Sichuan University for help with SEM characterization.

Characterization methods

CFs need to be cut as short as possible and ground into powder with KBr. The chemical groups on the surface of CFs were analyzed by FTIR spectrophotometer (FTIR, Nicolet 570, USA) from 500 to 4000 cm^{-1} using powder-pressed KBr tablets. Before the test, the CFs shall be stored in a vacuum oven at 80 °C for more than 24 h to eliminate the water on the surface of CFs.

Carbon fiber bundles were bonded to the glass sheet for the test. Raman spectrometer (Raman, Dilor, France) was adopted to check the surface structural features of CFs. Raman spectrometer uses a helium-neon laser to emit a laser with a wavelength of 633 nm and scanned the surface of CFs in the range of 500–3000 cm^{-1} through a grating of 600 gr/mm. And then the Gaussian function was used to fit the curve.

Scanning electron microscope (SEM, JSM-9600, JEOL, Japan) and atomic force microscope (AFM, MultiMode III, Bruker, Germany) were employed to detect the surface morphology and roughness of CFs.

Monofilament tensile test was performed based on the ASTM D3379-75 [69] https://www.sciencedirect.com/science/article/pii/S0032386117310297 - bib26, where made on Instron 5566 at a cross-head speed of 10 mm min^{-1} and the gauge length of 20 mm. Effective data was collected and analyzed base on the Weibull statistical method [70].

Contact angle tester (DSA, Kruss, Germany) was used to measure the contact angle between CF and water. Sprayed 0.1 pL ultrapure water onto the horizontally straight single fiber fixed on the sample stage, and record the whole process of the droplet contacting with the fiber. Through the droplet shape analysis, the water contact angle of the single fiber was calculated. The contact angle of the samples was determined along with the average value of five different positions [71].

The interlaminar shear strength (ILSS) of carbon fiber composites (length, width, and thickness of specimens: 25 mm × 6.5 mm × 2 mm) was evaluated by the three-point short-beam bending test according to ASTM D2344 standard. The tests were carried out on a universal testing machine (Instron5567, USA).

The IFSS values calculated from:Where P_b represents the maximum breaking load, b is the width of the specimen (mm) and h is the thickness of the specimen (mm).

References

[1] L. Gao, J.U. Surjadi, K. Cao, H. Zhang, P. Li, S. Xu, C. Jiang, J. Song, D. Sun, Y. Lu, Flexible fiber-shaped supercapacitor based on nickel–cobalt double hydroxide and pen ink electrodes on metallized carbon fiber, ACS Appl. Mater. Interfaces 9 (2017) 5409–5418.
[2] W.X. Zhu, Y. Zhang, J.D. Gong, Y.Y. Ma, J. Sun, T. Lo, J.L. Wang, Surface engineering of carbon fiber paper toward exceptionally high-performance and stable electrochemical nitrite sensing, ACS Sens. 4 (2019) 2980–2987.
[3] N.Y. Li, Y.G. Li, J. Jelonnek, G. Link, J. Gao, A new process control method for microwave curing of carbon fibre reinforced composites in aerospace applications, Compos. B Eng. 122 (2017) 61–70.
[4] M.S. Islam, Y. Deng, L.Y. Tong, S.N. Faisal, A.K. Roy, A.I. Minett, V.G. Gomes, Grafting carbon nanotubes directly onto carbon fibers for superior mechanical stability: towards next generation aerospace composites and energy storage applications, Carbon 96 (2016) 701–710.
[5] F. Meng, J. McKechnie, T. Turner, K.H. Wong, S.J. Pickering, Environmental aspects of use of recycled carbon fiber composites in automotive applications, Environ. Sci. Technol. 51 (2017) 12727–12736.
[6] S. Chand, Carbon fibers for composites, J. Mater. Sci. 35 (2000) 1303–1313.
[7] High performance graphene oxide/polyacrylonitrile composite pervaporation membranes for desalination applications, J. Mater. Chem. 3 (2015) 5140–5147.
[8] J. Schultz, L. Lavielle, C. Martin, The role OF the interface IN carbon-fiber epoxy composites, J. Adhes. 23 (1987) 45–60.
[9] M.G. Bader, J.E. Bailey, I. Bell, The effect of fibre-matrix interface strength on the impact and fracture properties of carbon-fibre-reinforced epoxy resin composites, J. Phys. D 6 (1973) 572.
[10] J. Schultz, L. Lavielle, C. Martin, The role of the interface in carbon fibre-epoxy composites, J. Adhes. 23 (1987) 45–60.
[11] B. Gao, R.L. Zhang, M.S. He, L.C. Sun, C.G. Wang, L. Liu, L.F. Zhao, H.Z. Cui, A. P. Cao, Effect of a multiscale reinforcement by carbon fiber surface treatment with graphene oxide/carbon nanotubes on the mechanical properties of reinforced carbon/carbon composites, Compos. Appl. Sci. Manuf. 90 (2016) 433–440.
[12] D. Mamalis, J.J. Murray, J. McClements, D. Tsikritsis, V. Koutsos, E.D. McCarthy, C.M.O. Bradaigh, Novel carbon-fibre powder-epoxy composites: interface phenomena and interlaminar fracture behaviour, Compos. B Eng. 174 (2019) 13.
[13] M. Zhao, L.H. Meng, L.C. Ma, L.N. Ma, X.B. Yang, Y.D. Huang, J.E. Ryu, A. Shankar, T.X. Li, C. Yan, Z.H. Guo, Layer-by-layer grafting CNTs onto carbon fibers surface for enhancing the interfacial properties of epoxy resin composites, Compos. Sci. Technol. 154 (2018) 28–36.
[14] K. Naito, J.M. Yang, Y. Tanaka, Y. Kagawa, The effect of gauge length on tensile strength and Weibull modulus of polyacrylonitrile (PAN)- and pitch-based carbon fibers, J. Mater. Sci. 47 (2012) 632–642.
[15] L.C. Pardini, L.G.B. Manhani, Influence of the testing gage length on the strength, young's modulus and Weibull modulus of carbon fibres and glass fibres, Mater. Res. 5 (2002) 411–420.
[16] C.L. Weitzsacker, M. Xie, L.T. Drzal, Using XPS to investigate fiber matrix chemical interactions in carbon-fiber-reinforced composites, Surf. Interface Anal. 25 (1997) 53–63.
[17] H. Kazan, T. Zheng, S. Farahani, S. Pilla, Degree of cure, mechanical properties, and morphology of carbon fiber/epoxy- PP hybrids manufactured by a novel single shot method, Mater. Today Commun. 19 (2019) 441–449.
[18] A. Bismarck, C. Wuertz, J. Springer, Basic surface oxides on carbon fibers, Carbon 37 (1999) 1019–1027.
[19] F.-h. Shi, Z.-s. Dai, B.-y. Zhang, Characterization of surface properties of carbon fibers and interfacial properties of carbon fibers reinforced matrix composites, J. Aeronautical Mater. 30 (2010) 43–47.
[20] K. Naito, J.M. Yang, Y. Inoue, H. Fukuda, The effect of surface modification with carbon nanotubes upon the tensile strength and Weibull modulus of carbon fibers, J. Mater. Sci. 47 (2012) 8044–8051.
[21] Q. Wu, R.Y. Zhao, J.F. Zhu, F. Wang, Interfacial improvement of carbon fiber reinforced epoxy composites by tuning the content of curing agent in sizing agent, Appl. Surf. Sci. 504 (2020) 12.
[22] L.C. Ma, Y.Y. Zhu, P.F. Feng, G.J. Song, Y.D. Huang, H. Liu, J.X. Zhang, J.C. Fan, H. Hou, Z.H. Guo, Reinforcing carbon fiber epoxy composites with triazine derivatives functionalized graphene oxide modified sizing agent, Compos. B Eng. 176 (2019) 10.
[23] F.Y. Liu, Z. Shi, Y.B. Dong, Improved wettability and interfacial adhesion in carbon fibre/epoxy composites via an aqueous epoxy sizing agent, Compos. Appl. Sci. Manuf. 112 (2018) 337–345.
[24] A. Hendlmeier, L.I. Marinovic, S. Al-Assafi, F. Stojcevski, L.C. Henderson, Sizing effects on the interfacial shear strength of a carbon fibre reinforced two-component thermoplastic polymer, Compos. Appl. Sci. Manuf. 127 (2019) 9.
[25] Z.Y. Wang, H.J. Guo, H. Zhou, X.F. Ouyang, D. Jiang, J.H. Li, Q.P. Guo, J. Tang, C. C. Yang, Effect of the chain structure of self-emulsifying polyester sizing agent on ILSS of carbon fiber/unsaturated polyester resin composites, Polymers 11 (2019) 15.
[26] Y.P. Fu, H.X. Li, W.Y. Cao, Enhancing the interfacial properties of high-modulus carbon fiber reinforced polymer matrix composites via electrochemical surface oxidation and grafting, Compos. Appl. Sci. Manuf. 130 (2020) 11.
[27] A. Karakassides, A. Ganguly, K. Tsirka, A.S. Paipetis, P. Papakonstantinou, Radially grown graphene nanoflakes on carbon fibers as reinforcing interface for polymer composites, ACS Applied Nano Materials 3 (2020) 2402–2413.
[28] L. Feng, K.Z. Li, Z.S. Si, Q. Song, H.J. Li, J.H. Lu, L.J. Guo, Compressive and interlaminar shear properties of carbon/carbon composite laminates reinforced with carbon nanotube-grafted carbon fibers produced by injection chemical vapor deposition, Mater. Sci. Eng. A-Struct. Mater. Prop. Microstruct. Process. 626 (2015) 449–457.
[29] L.B. Zheng, Y.X. Wang, J.J. Qin, X.H. Wang, R.J. Lu, C. Qu, C.G. Wang, Scalable manufacturing of carbon nanotubes on continuous carbon fibers surface from chemical vapor deposition, Vacuum 152 (2018) 84–90.
[30] M. Delamar, G. Desarmot, O. Fagebaume, R. Hitmi, J. Pinson, J.M. Saveant, Modification of carbon fiber surfaces by electrochemical reduction of aryl diazonium salts: application to carbon epoxy composites, Carbon 35 (1997) 801–807.
[31] N.T. Tran, B.A. Patterson, A.G. Kolodziejczyk, V.M. Wu, D.B. Knorr, Electrochemical surface treatment of discontinuous carbon fibers, Langmuir 35 (2019) 12374–12388.
[32] J.J. Jiang, X.M. Yao, C.M. Xu, Y. Su, L.C. Zhou, C. Deng, Influence of electrochemical oxidation of carbon fiber on the mechanical properties of carbon fiber/graphene oxide/epoxy composites, Compos. Appl. Sci. Manuf. 95 (2017) 248–256.
[33] H. Lee, I. Ohsawa, J. Takahashi, Effect of plasma surface treatment of recycled carbon fiber on carbon fiber-reinforced plastics (CFRP) interfacial properties, Appl. Surf. Sci. 328 (2015) 241–246.
[34] M.B. Borooj, A.M. Shoushtari, A. Haji, E.N. Sabet, Optimization of plasma treatment variables for the improvement of carbon fibres/epoxy composite performance by response surface methodology, Compos. Sci. Technol. 128 (2016) 215–221.
[35] J. Moosburger-Will, E. Lachner, M. Loffler, C. Kunzmann, M. Greisel, K. Ruhland, S. Horn, Adhesion of carbon fibers to amine hardened epoxy resin: influence of ammonia plasma functionalization of carbon fibers, Appl. Surf. Sci. 453 (2018) 141–152.

[36] X.M. Yuan, B. Zhu, X. Cai, K. Qiao, S.Y. Zhao, J.W. Yu, Influence of different surface treatments on the interfacial adhesion of graphene oxide/carbon fiber/epoxy composites, Appl. Surf. Sci. 458 (2018) 996–1005.
[37] J.D.H. Hughes, The carbon-fiber epoxy interface - a review, Compos. Sci. Technol. 41 (1991) 13–45.
[38] Y.S. Lee, B.K. Lee, Surface properties of oxyfluorinated PAN-based carbon fibers, Carbon 40 (2002) 2461–2468.
[39] S.J. Park, J.S. Kim, Influence of plasma treatment on microstructures and acid–base surface energetics of nanostructured carbon blacks: N2 plasma environment, J. Colloid Interface Sci. 244 (2001) 336–341.
[40] J.S. Park, H.S. Kim, H.T. Hahn, Healing behavior of a matrix crack on a carbon fiber/mendomer composite, Compos. Sci. Technol. 69 (2009) 1082–1087.
[41] Y.L. Ji, C.X. Lu, P.C. Zhou, Y. Yang, X.X. Lu, Y.H. Li, S.X. Yuan, F. He, Effect of a Ni-P coating on the tensile strength of carbon fibers evaluated by a Weibull statistical method, N. Carbon Mater. 23 (2008) 159–164.
[42] W.W. Jiao, Y.M. Cai, W.B. Liu, F. Yang, L. Jiang, W.C. Jiao, R.G. Wang, Preparation of carbon fiber unsaturated sizing agent for enhancing interfacial strength of carbon fiber/vinyl ester resin composite, Appl. Surf. Sci. 439 (2018) 88–95.
[43] S. Rudzinski, L. Haussler, C. Harnisch, E. Mader, G. Heinrich, Glass fibre reinforced polyamide composites: thermal behaviour of sizings, Compos. Appl. Sci. Manuf. 42 (2011) 157–164.
[44] R.L. Zhang, Y.D. Huang, L. Liu, Y.R. Tang, D. Su, L.W. Xu, Effect of emulsifier content of sizing agent on the surface of carbon fibres and interface of its composites, Appl. Surf. Sci. 257 (2011) 3519–3523.
[45] R.K. Layek, A. Kundu, A.K. Nandi, High-performance nanocomposites of sodium carboxymethylcellulose and graphene oxide, Macromol. Mater. Eng. 298 (2013) 1166–1175.
[46] D. Pasqui, P. Torricelli, M. De Cagna, M. Fini, R. Barbucci, Carboxymethyl cellulose-hydroxyapatite hybrid hydrogel as a composite material for bone tissue engineering applications, J. Biomed. Mater. Res. 102 (2014) 1568–1579.
[47] M. Saqib, I. Khan, S. Shafie, Application of Atangana-Baleanu fractional derivative to MHD channel flow of CMC-based-CNT's nanofluid through a porous medium, Chaos, Solit. Fractals 116 (2018) 79–85.
[48] L.B. Dong, Q. Yang, C.J. Xu, Y. Li, D.M. Yang, F. Hou, H.F. Yin, F.Y. Kang, Facile preparation of carbon nanotube aerogels with controlled hierarchical microstructures and versatile performance, Carbon 90 (2015) 164–171.
[49] C. Wang, M. Zhao, J. Li, J. Yu, S. Sun, S. Ge, X. Guo, F. Xie, B. Jiang, E.K. Wujcik, Silver nanoparticles/graphene oxide decorated carbon fiber synergistic reinforcement in epoxy-based composites, Polymer, 131 263-271.
[50] Z.T. Hou, M.Q. Sun, B. Li, X.D. Zhang, A New Method to Prepare Carbon Fiber/Carbon Black Reinforced Concrete and its Properties, Adv. Mater. Res., 168-170 1077-1081.
[51] Y.R. Son, S.J. Park, Green preparation and characterization of graphene oxide/carbon nanotubes-loaded carboxymethyl cellulose nanocomposites, Sci. Rep. 8 (2018) 10.
[52] A. Hajian, Q. Fu, L.A. Berglund, Recyclable and superelastic aerogels based on carbon nanotubes and carboxymethyl cellulose, Compos. Sci. Technol. 159 (2018) 1–10.
[53] T. Sun, H.W. Zou, Y. Zhou, R. Li, M. Liang, Y. Chen, Achieving high-performance epoxy nanocomposites with trifunctional poly(oxypropylene)amines functionalized graphene oxide, High Perform. Polym. 31 (2019) 557–569.
[54] Z.Q. Rao, H.Y. Ge, L.L. Liu, C. Zhu, L. Min, M. Liu, L.H. Fan, D. Li, Carboxymethyl cellulose modified graphene oxide as pH-sensitive drug delivery system, Int. J. Biol. Macromol. 107 (2018) 1184–1192.
[55] Y.L. Zhang, Y. Liu, X.R. Wang, Z.M. Sun, J.K. Ma, T. Wu, F.B. Xing, J.P. Gao, Porous graphene oxide/carboxymethyl cellulose monoliths, with high metal ion adsorption, Carbohydr. Polym. 101 (2014) 392–400.
[56] B. Gao, J. Zhang, Z.N. Hao, L.J. Huo, R.L. Zhang, L. Shao, In-situ modification of carbon fibers with hyperbranched polyglycerol via anionic ring-opening polymerization for use in high-performance composites, Carbon 123 (2017) 548–557.
[57] L. Liu, F. Yan, M. Li, M.J. Zhang, L.H. Xiao, L. Shang, Y.H. Ao, Improving interfacial properties of hierarchical reinforcement carbon fibers modified by graphene oxide with different bonding types, Compos. Appl. Sci. Manuf. 107 (2018) 616–625.
[58] J.S. Fu, M.J. Zhang, L. Jin, L. Liu, N. Li, L. Shang, M. Li, L.H. Xiao, Y.H. Ao, Enhancing interfacial properties of carbon fibers reinforced epoxy composites via Layer-by-Layer self assembly GO/SiO2 multilayers films on carbon fibers surface, Appl. Surf. Sci. 470 (2019) 543–554.
[59] J.F. Xie, D.W. Xin, H.Y. Cao, C.T. Wang, Y. Zhao, L. Yao, F. Ji, Y.P. Qiu, Improving carbon fiber adhesion to polyimide with atmospheric pressure plasma treatment, Surf. Coating. Technol. 206 (2011) 191–201.
[60] D.M. Che, I. Saxena, P.D. Han, P. Guo, K.F. Ehmann, Machining of carbon fiber reinforced plastics/polymers: a literature review, J. Manuf. Sci. Eng.-Trans. ASME 136 (2014) 22.
[61] P.W. Beaumont, B. Harris, Energy OF crack-propagation IN carbon fiber-reinforced resin systems, J. Mater. Sci. 7 (1972) 1265.
[62] K.L. Pickering, T.L. Murray, Weak link scaling analysis of high-strength carbon fibre, Compos. Appl. Sci. Manuf. 30 (1999) 1017–1021.
[63] A.A. Griffith, The Phenomena of Rupture and Flow in Solids, 1921.
[64] J. Jortner, Macroporosity and interface cracking in multi-directional carbon-carbons, Carbon 24 (1986) 603–613.
[65] T. Ogawa, M. Ikeda, Determination of the contact angle of a liquid droplet on a carbon fiber, J. Adhes. 43 (1993) 69–78.
[66] X. Chen, H.B. Xu, D. Liu, C. Yan, Y.D. Zhu, A facile one-pot fabrication of polyphosphazene microsphere/carbon fiber hybrid reinforcement and its effect on the interfacial adhesion of epoxy composites, Appl. Surf. Sci. 410 (2017) 530–539.
[67] X.Q. Zhang, X.Y. Fan, C. Yan, H.Z. Li, Y.D. Zhu, X.T. Li, L.P. Yu, Interfacial microstructure and properties of carbon fiber composites modified with graphene oxide, ACS Appl. Mater. Interfaces 4 (2012) 1543–1552.
[68] L. Szabo, S. Imanishi, F. Tetsuo, D. Hirose, H. Ueda, T. Tsukegi, K. Ninomiya, K. Takahashi, Lignin as a functional green coating on carbon fiber surface to improve interfacial adhesion in carbon fiber reinforced polymers, Materials 12 (2019) 15.
[69] A. D3379-75, Standard Test Method for Tensile Strength and Young's Modulus for High-Modulus Single-Filament Materials, 1975.
[70] W. Weibull, A statistical distribution function of wide applicability, J. Appl. Mech.-Trans. ASME 18 (1951) 293–297.
[71] Y.Q. Li, C. Zou, J.Z. Shao, X.W. Zhang, Y.N. Li, Preparation of SiO2/PS superhydrophobic fibers with bionic controllable micro-nano structure via centrifugal spinning, RSC Adv. 7 (2017) 11041–11048.